



Tipping point analysis helps identify sensor phenomena in humidity data

Valerie N. Livina¹, Kate Willett², and Stephanie Bell¹

¹National Physical Laboratory, Teddington, UK

²Met Office, Exeter, UK

Correspondence: Valerie N. Livina (valerie.livina@npl.co.uk)

Abstract. Humidity variables are important for monitoring climate. Unlike, for instance, temperature, they require data transformation to derive water vapour variables from observations. Hygrometer technologies have changed over the years and, in some cases, have been prone to sensor drift due to aging, condensation or contamination in service, requiring replacement. Analysis of these variables may provide rich insight into both instrumental and climate dynamics. We apply tipping point analysis to dew point and relative humidity values from hygrometers at 55 observing stations in the UK. Our results demonstrate these techniques, which are usually used for studying geophysical phenomena, are also potentially useful for identifying historic instrumental changes that may be undocumented or lack metadata.

1 Introduction

Studying climate variables requires complex measurements and transformations of data. During the period of a given continuous record, observations may be derived from successive instruments. Sensors may undergo multiple technical changes, from replacements of instruments to drifts and degradation. Detecting such changes, especially during earlier periods of deployment, which were not fully documented, is an important task that contributes to better interpretation of data that forms climate records — in particular, to enable homogenisation processes that identify and address inconsistent data (Menne and Williams, 2009; Peterson et al, 1998). Homogenisation, detection of changes, and recovery of missing metadata also contribute to generic FAIR data principles: Findable, Accessible, Interoperable, and Reusable. In particular, it is necessary to produce robust long-term analyses to assess climate change, that changepoint detection at monthly timescales is relative well established (Reeves et al, 2007). However, as now we move into an era of high-frequency and global-coverage climate services, there is the need for robust daily and even hourly analyses to assess extreme events, their intensity and frequency (Trewin, 2013; Brugnara et al, 2023). This makes monitoring climate sensor networks and their quality particularly important.

It is known that manual observations were replaced by automatic ones, and that many analogue instruments were replaced by digital ones at various stages of environmental observations. Some of these changes were not fully documented, or the records are not now accessible. Some instrument types have exhibited significant drift during period of service in between checks, electronic hygrometers being one example. Furthermore, a station may have moved (yet its metadata identifies it as at the same



location) or instruments re-situated within the station grounds, or the local environment may have changed (urbanisation, city
25 to airport, agricultural practices, afforestation or deforestation).

Therefore, it is important to analyse environmental records using suitable data techniques that are able to detect such artefacts
and distinguish them from the natural phenomena being observed. In this article, we study humidity records of several decades
using tipping point analysis that is capable of detecting long-term natural phenomena, such as climate change, as well as abrupt
changes of data patterns caused by technical artefacts. This is the first time that tipping point analysis is deployed for such a
30 purpose, and we demonstrate its usability for detection of instrumental changes. If used in real-time, utilising a small window
size for up-to-now available data (thus reducing uncertainty in timing the change), tipping point analysis may help identify
drifting of sensors and, in principle, prevent prolonged recording of poor-quality data. If used for historic datasets, a change in
the noise characteristics might help identify a change in technology (for example from psychrometer to electronic hygrometer)
in cases where this might not otherwise be recorded or detectable. Improving such information can potentially improve the
35 attribution of uncertainty in cases where only a worst-case uncertainty might otherwise be assigned.

2 Methodology

2.1 Overview of method

In the work reported here, the technique more conventionally used to identify tipping points of complex systems was applied
to several time series of near-surface observations of air temperature and of humidity at UK locations. After potential change
40 points were identified using the analysis, the observation records and their metadata were assessed to investigate whether the
identified change points corresponded to significant events such as the change of an instrument or of a recording technique.

2.2 Tipping Point Analysis

After Poincaré's pioneering work on bifurcation theory Poincaré (1892), in the 1960s and 1970s an intuitive idea of a bifurcation
appeared in social sciences as the term 'tipping point' coined by sociologists. Malcolm Gladwell published a bestselling book
45 on tipping points (Gladwell, 2000), where he expanded the approach to biophysical systems. In 2008, Lenton et al. published
the seminal paper on tipping elements in the Earth system (Lenton et al, 2008), in which the main geophysical tipping elements
were described. Lenton's work gave an onset to multiple publications in geophysics and paleoclimate, focussing on early-
warning signals (EWS) of tipping points (Livina, 2023). Applications of tipping point analysis have been found in geophysics
(Lenton et al, 2008; Livina et al, 2011, 2010, 2013), statistical physics (Vaz Martins et al, 2010), ecology (Dakos et al, 2012),
50 structure health monitoring (Livina et al, 2014) and failure dynamics in semiconductors (Livina et al, 2020). Most of these
studies were focussed on long-range changes in dynamical systems, such as climate change, or on engineering phenomena,
such as failures of devices or installations. In this paper, we return to geophysical applications, but with the purpose of studying
sensor conditions, which bridges the gap between such applications and broadens the scope of tipping point analysis. We also
supplement the analysis with a Bayesian estimate of significance of changes, which we illustrate on humidity data.



55 We propose to use the tipping observed in fluctuations (changes in the patterns of a dataset noise, which are not necessarily in the form of a geophysical tipping point) to identify changes in the patterns of the instrumental data, attributable to changes of the instrument or the observing technique.

The basis of the EWS in tipping point analysis is monitoring changes of patterns in fluctuations using approximating stochastic models. Such models are powerful yet simple tools for modelling time series of real-world dynamical systems. Given a one-dimensional trajectory of a dynamical system (the recorded time series), the system dynamics can be modelled by the stochastic equation with state variable z and time t :

$$\dot{z} = D(z, t) + S(z, t), \quad (1)$$

where \dot{z} is the time derivative of the system variable $z(t)$, and D and S are deterministic and stochastic components, respectively. Component $D(z, t)$ may be stationary or dynamically changing (for instance, containing long-term or periodic trends or both).

The tipping-point analysis consists of the following three stages: 1) anticipating (pre-tipping, or EWS detection/analysis), 2) detecting (tipping), and 3) forecasting (post-tipping). For the purpose of the current analysis, we use only the first stage of the tipping point analysis: anticipation, or early-warning signal.

Anticipating tipping points (pre-tipping) is based on the effect of critical slowing down of the dynamics of the system prior to critical behaviour, i.e., increasing return time to equilibrium (Wissel, 1984). When a system state becomes unstable and starts a transition to another state, the response to small perturbations becomes slower. This “critical slowing down” can be detected as increasing autocorrelations (ACF) in the time series (Held and Kleinen, 2004). Alternatively, the short-range scaling exponent of Detrended Fluctuation Analysis (DFA) (Peng et al, 1994) may be monitored (Livina and Lenton, 2007). The lag-1 autocorrelation (Brockwell and Davis, 2016) is the value of the autocorrelation function at lag=1, the autocorrelation function being the average dependence between elements of time series at various steps, or lags. Lag-1 ACF is calculated in sliding windows of fixed length (conventionally, half of the series length) or variable length (for uncertainty estimation) along the time series, which produces a curve of an early-warning indicator. This indicator describes the structural dynamics of the time series. If the curve of the indicator remains flat and stable, the time series does not undergo a critical change (whether bifurcational or transitional). If the indicator rises to a critical value of 1 (the monotonic trend can be estimated, for instance, using Kendall rank correlation), it provides a warning of critical behaviour.

Lag-1 autocorrelation is estimated by fitting an autoregressive process of order 1 (AR1), which is a common modelling tool in time series analysis:

$$z_{t+1} = cz_t + \sigma\eta_t \quad (2)$$

where η_t is a Gaussian white noise process of unit variance, σ is the noise level as a standard deviation, and $c = e^{-\kappa\Delta t}$ is the ‘ACF-indicator’ with κ the decay rate of perturbations. Then, $c \rightarrow 1$ as $\kappa \rightarrow 0$ when a tipping point is approached. In addition, the DFA method utilises built-in detrending of a chosen polynomial order, which allows transitions and bifurcations to be distinguished in the EWS. These features can be identified by comparing several early-warning indicators, with and without



detrending data in sliding windows (Livina et al, 2012). The paper of Livina and Lenton (2007) provided the first application of the DFA-based early-warning indicator to the paleotemperature record with detected transition using both ACF and DFA indicators.

Detection of a tipping point is performed using dynamical potential analysis. The technique detects a bifurcation in a time series and the time when it happens, which is illustrated in a potential plot mapping by colour the potential dynamics of the system (Livina et al, 2011, 2010). The technique of potential **forecasting** is based on dynamical propagation of the probability density function of the time series (Livina et al, 2013).

The theory of tipping point analysis is generic, and here it is useful for detection, for example, of such cases where a hygrometer progressively under-reads (locally indistinguishable from true value), then a site check establishes that the instrument is out of specification, and it is replaced with a new calibrated hygrometer. In data, such a change would look like a local step-change in the data that follows some drifting trend (this trend may have provided a short EWS). Another case could be that a wet- and dry-bulb hygrometer read a few times per day is replaced with an electronic sensor (that reads at the same temporal intervals), which is then replaced by an automated reading protocol logged at 1-minute intervals (these datasets might have different effective resolution, or different error (noise) characteristics). Such a change of sampling rate would immediately produce stronger auto-correlations in the data, which would be detectable using the lag-1 autocorrelation EWS technique. We are also interested to detect more complex instrument changes, such as station/instrument moves, instrument drifts, and various local environment changes.

2.3 Humidity measurements

Following (Willett et al, 2014), calculation of relative humidity in this work is based on several input and derived variables as follows:

$$\begin{aligned} \text{Vapour pressure with respect to water } (e) \text{ in hectopascals} \quad & e = 6.1121 \cdot f_w \cdot \exp\left(\frac{\left(18.729 - \left(\frac{T_d}{227.3}\right)\right)T_d}{257.87 + T_d}\right) \\ & f_w = 1 + 7 \times 10^{-4} + 3.46 \times 10^{-6} P_{\text{mst}} \\ \text{Vapour pressure with respect to ice } (e_{\text{ice}}) \text{ in hectopascals} \quad & e_{\text{ice}} = 6.1121 \cdot f_i \cdot \exp\left(\frac{\left(23.036 - \left(\frac{T_d}{333.7}\right)\right)T_d}{279.82 + T_d}\right) \\ & f_i = 1 + 3 \times 10^{-4} + 4.18 \times 10^{-6} P_{\text{mst}} \\ \text{Station pressure } (P_{\text{mst}}) \text{ in hectopascals} \quad & P_{\text{mst}} = P_{\text{msl}} \left(\frac{T}{T + 0.0065Z}\right)^{5.625} \\ \text{Relative humidity (RH) in percent relative humidity} \quad & RH = 100 \left(\frac{e}{e_s}\right), \end{aligned} \tag{3}$$

where T is station climatological monthly mean, T_d is dew-point temperature (in Kelvins), P_{msl} is pressure at mean sea level, Z is height in metres, e_s is saturated vapour pressure.



3 Data

We consider humidity observations in the UK that span several decades, which have been gathered by the UK Met Office. Initially, datasets of 56 stations were provided, many of them with large gaps. After removing data before the largest gap, 55 stations were selected, although some of the records became very short after the gap-based truncation. Filling large gaps with
115 interpolated data would affect autocorrelations and thus introduce undesirable bias in early-warning indicators, which would distort searches for instrumental changes in the data.

Using the dewpoint variable and pressure variable from the ECMWF ERA-5 (European Centre for Medium-Range Weather
Forecasts, Reanalysis v5) data for the considered area (Hersbach et al, 2020) (the reanalysis pressure variable, after necessary
temporal interpolation, being an acceptable approximation for the purposes of our data processing), we obtained the relative
120 humidity using equations (3).

Dewpoint and relative humidity datasets were pre-processed as follows:

- Where large gaps were observed, the initial part of the data that included the gap was removed
- Global trend and seasonality were removed using singular spectrum analysis (Broomhead and King, 1986) from both dewpoint and relative humidity variables.
- 125 – Detrended fluctuations of dewpoint and relative humidity were analysed using lag-1 ACF for EWS for the purpose of detecting instrumental changes. The strength of the EWS trend was quantified using the Mann-Kendall coefficient for assessment of monotonous trend (ideally increasing trend gives Kendall value 1, ideally decreasing -1). For the considered 55 stations, averaged Kendall values of dewpoint detrended fluctuations are 0.30 ± 0.54 , whereas for relative humidity detrended fluctuations, the Kendall values are 0.68 ± 0.44 (mean and standard error). This is summarised in
130 Fig. 1.

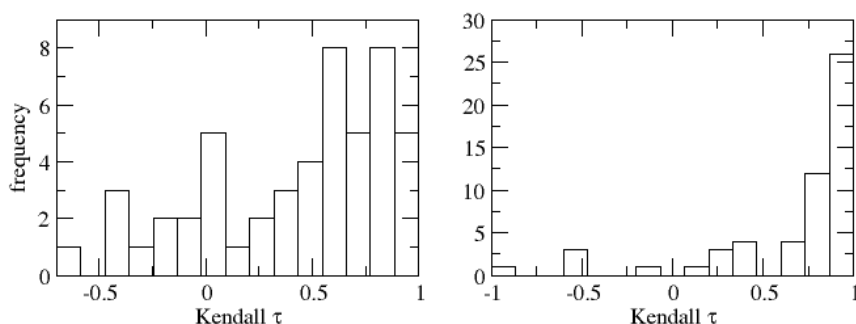


Figure 1. Histograms of Mann-Kendall coefficients of monotonic trends in early-warning indicators for dewpoint (left panel) and relative humidity (right panel). High positive values of the coefficient denote significant increasing trend indicating EWS.



Significant negative trends in both variables were observed in datasets for the locations of Leeming, Fylingdales, Lyneham, Jersey. Such effects in early-warning indicators may denote stabilisation (opposite to a critical transition), which may be, for example, due to urban effects on the instruments, such as loss of shrubs and building up of green areas.

Autocorrelations were analysed using a short single window. Conventionally, a much larger window size is used for tipping point analysis, as the phenomenon of interest in geophysics is usually of longer scale (decades), often related to climate change. In this case, we need to consider short-term events (replacement of an instrument or its drift/calibration, station moves, local environment changes), and a short window with a smaller subset of data for averaging provide higher sensitivity for the purpose of our analysis. The size of the sliding window should be selected in such a way that high-frequency fluctuations (which produce maximal lag-1 autocorrelations) would be smoothened out, whereas intrinsic EWS would be detected (usually increasing in the interval $[0.7, 1]$ — see the examples in the Appendix). The choice of window can be explored and furthermore automated using statistical techniques (such as scaling analysis with long-term exponents), because each geophysical variable has signature scaling behaviour, and therefore need to be investigated individually. In this case study, we note that we have selected a suitably small window size, which produced detectable EWS for the purposes of our analysis. In general, the smaller the window size, the better for studying sensor phenomena, as we want to identify nonstationarities, possibly caused by instrumental artefacts and sometimes reversed short-term transitions (for example, transient extreme events). In principle, it is possible to study the same time series with different windows of early-warning indicators, for different purposes: shortest one to identify instrument replacement, and longer one for studying environmental changes, such as encroachment of town or forest.

Spatial distribution of the detected long-term changes in the EWS indicators across the UK for relative humidity is mapped according to the Mann-Kendall coefficient for detection of monotonous trends, which is illustrated in Fig. 2. This plot shows where the long-term changes in humidity are more pronounced (large blue dots), and this can be further analysed in terms of local micro-climates and city/country distributions.

We consider the Bingley station (Midlands countryside) as a representative example for detailed analysis. It is known that there was a period of instrumental changes in environmental sensors. For example, in the 1980s-1990s there were replacements of the earlier analogue instruments with modern digital, which can be detected using ACF-based indicators of the tipping point analysis. Figure 3 illustrates at a glance such a clear change. It is interesting that the probability density functions of dew point and RH have different shapes (skewness), probably due to the nonlinearity of the equations linking them, as can be seen in Fig. 4. Autocorrelation functions differ, too, which reflects memory in the data (i.e., internal dependencies between the points of time series), as can be seen in Fig. 5.

To perform automatic identification of instrumental changes, one can use probabilistic estimation of change points in the EWS indicators. By applying the Matlab package “Bayesian Changepoint Detection & Time Series Decomposition” (Zhao et al, 2019), we identify change points in EWS indicators, specifically those of statistical significance. As can be seen in the following plots, the changes in the indicators that are statistically significant can be identified in the probabilities of the changes based on the Bayesian ensembles with Monte Carlo simulations (Zhao et al, 2019). The considered variable was detrended relative humidity, for which the ACF-indicator was calculated, which then was analysed using the Bayesian model

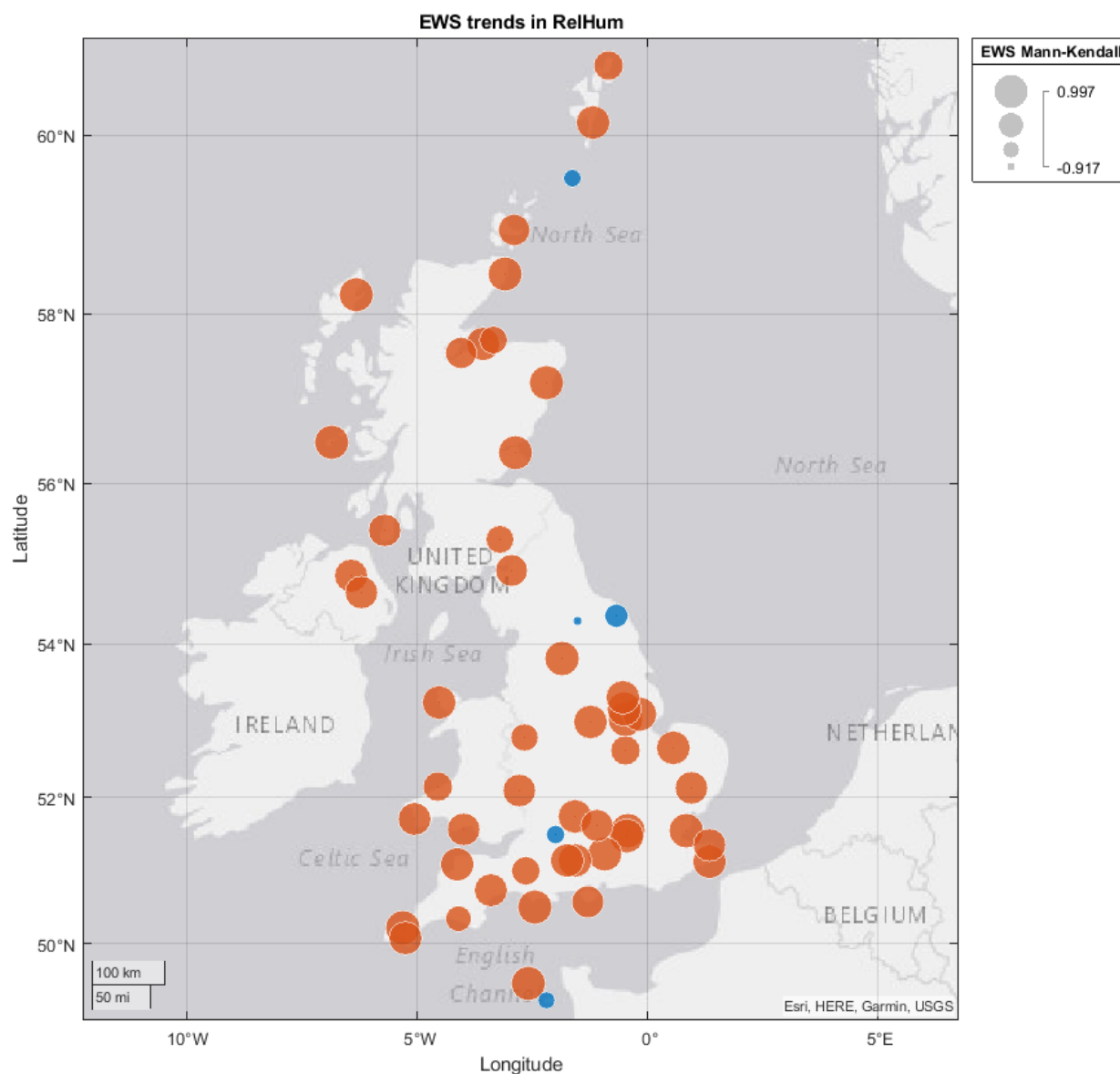


Figure 2. Spatial mapping of linear trends in EWS indicators for the detrended fluctuations of relative humidity in the UK. Trends were fitted over the whole range of each indicator, size of dot is defined by the value of the lead coefficient, and the colour denotes direction of trend (red — positive, blue — negative).

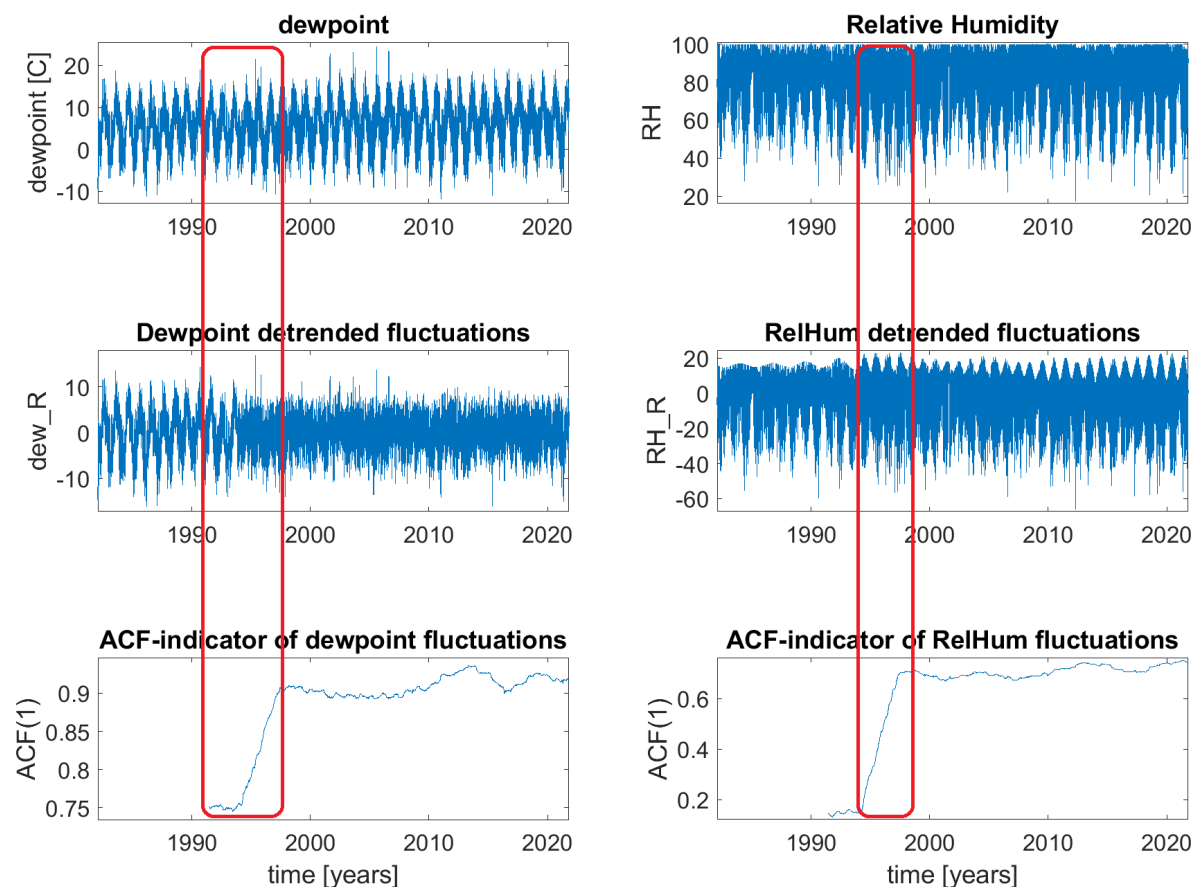


Figure 3. Bingley dew point and relative humidity (upper panels), their detrended fluctuations (middle panels) and EWS indicators calculated with 10% sliding windows. Clear trends in indicators show transitional behaviour — likely instrumental change in 1995.

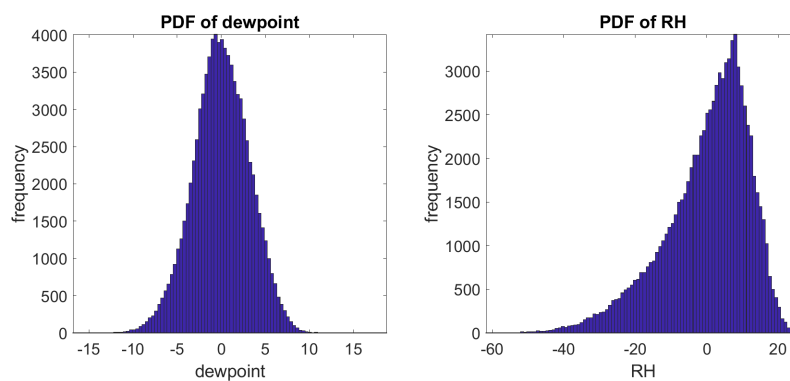


Figure 4. Histograms of the Bingley dew point and relative humidity.

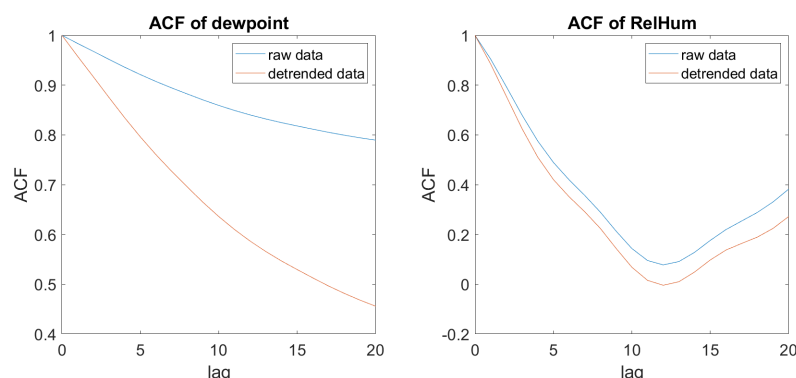


Figure 5. Autocorrelation functions of the Bingley dew point and relative humidity, with and without detrending.

165 ensemble. The changes with statistically significant peaks (probability >0.8) are narrow, and the timing of change events can be identified with small uncertainty of several weeks, if necessary.

In the case of Bingley, there are two statistically significant changes, in 1994 and in 1998, which are indicated in the lower panel with probabilities of changes, see Fig. 6. The red dots in the upper panels denote the recorded changes of operations (this data was provided by Met Office for verification), for which the major changes from manual to automatic were detected by the
170 abrupt increases in indicators. The introduced method of instrumental recording changed the patterns of autocorrelations, and this is detectable by the EWS indicators. In the later period, short intermittencies did not affect the indicators as much as the major change of the technology in the 1990s, yet many of them can be seen in the probabilistic detections in the bottom panel of Fig. 6.

In further discussions of the known instrument changes, it was mentioned that in Bingley, in 1994 and 1996, there were
175 changes from manual to automatic, as well as a change of the local airfield, which is an excellent confirmation of the detected abrupt transition. Moreover, the smaller detections in the years 2007, 2011, 2018 were reported to be related to routine replacements of sensors at Bingley. This demonstrates the capability of these techniques in sensitive detection of instrumental change.

For comparison, we plot equivalent results for stations Camborne (Fig. 7) and Carlisle (Fig. 8). We note that both of these
180 analyses show strong detections of changes in the 1980s and 1990s.

The results of the analysis of the changes in the indicators for relative humidity for the large set of 55 observing stations are summarised in the supplementary Table in the Appendix. Abrupt changes in EWS indicators are likely to be instrumental, whereas gradual ones are likely to be climatic (either natural, such as long-term climate change, or anthropogenic, such as urbanisation and change of local environment). The reported detections were later confirmed by available records of instrumental
185 changes for some of the stations.

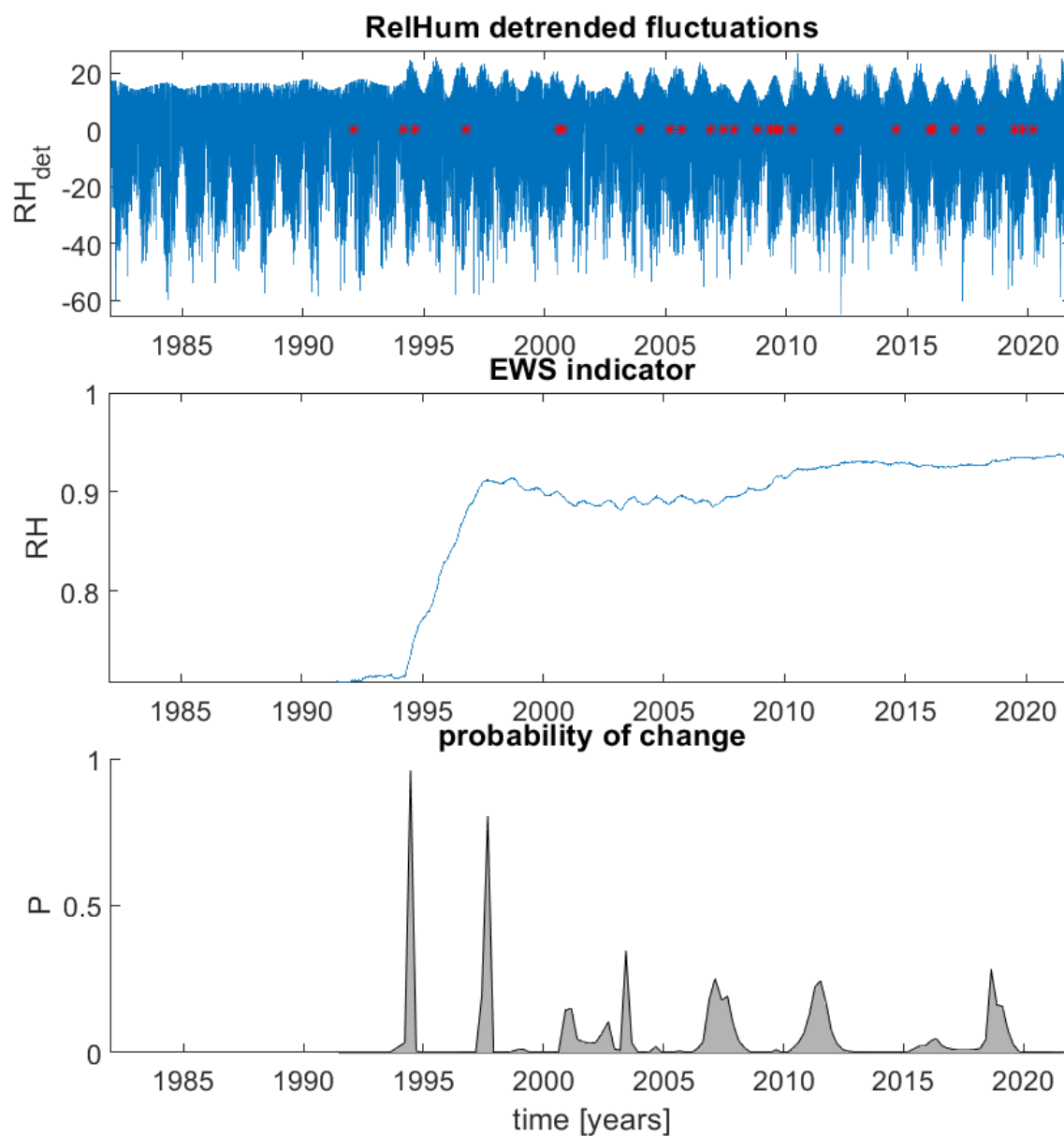


Figure 6. Bingley detrended (det) fluctuations of relative humidity with red dots denoting the recorded changes of operations (upper panel), its ACF-indicator with a small window, which is suitable for detection of instrumental changes with change of fluctuation patterns (middle panel), and Bayesian analysis of the indicator curve, which denotes probabilities of changes (lower panel).

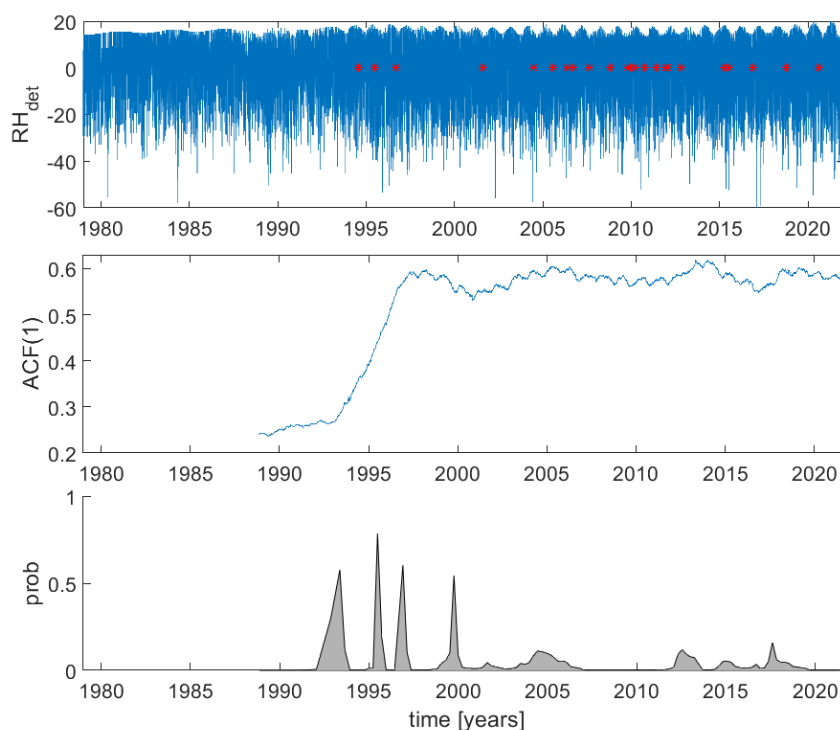


Figure 7. Camborne detrended (det) fluctuations of relative humidity with red dots denoting the recorded changes of operations (upper panel), its ACF-indicator with a small window, which is suitable for detection of instrumental changes with change of fluctuation patterns (middle panel), and Bayesian analysis of the indicator curve, which denotes probabilities of changes (lower panel).

4 Conclusion

We have applied tipping point analysis in a novel way (compared with its conventional use) to study instrumental and sensor phenomena in a large UK dataset of relative humidity. We carefully preprocessed the data to ensure that no underlying trends would affect the results, and as a consequence we have been able to reveal signatures of sensor events and phenomena.

190 In many of the stations, when applying a small sliding window, various transitions were observed. In particular, in the mid-1980s and mid-1990s, the tipping point analysis identified several rapid transitions, which are likely to have been caused by instrumental artefacts, based on the verification from the station records. In other cases, transitions are gradual, and often reversed later. Such reversal changes may be related to local stabilisation of environmental conditions.

In this paper, we analysed dewpoint and relative humidity, which are observed variables that require multiple stages of processing. We identified short-term instrumental effects in the data using early-warning indicators of the tipping point analysis. 195 These techniques are useful in identifying instrumental changes in those cases, when documentation and historical metadata

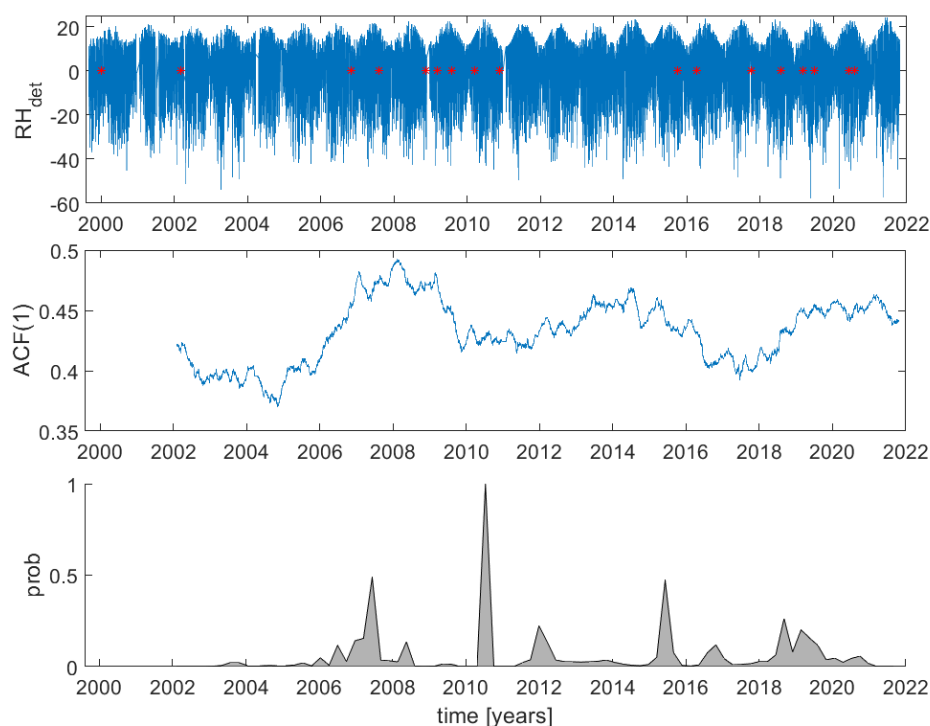


Figure 8. Carlisle detrended (det) fluctuations of relative humidity with red dots denoting the recorded changes of operations (upper panel), its ACF-indicator with a small window, which is suitable for detection of instrumental changes with change of fluctuation patterns (middle panel), and Bayesian analysis of the indicator curve, which denotes probabilities of changes (lower panel).

may be missing. This demonstration of the application of the early-warning signal techniques is new and supplementary to their conventional use of tipping point analysis in climatology and geophysics.

The observed effects are not climatic tipplings, but rather an example of short-term critical transitions caused by instrumental modifications and/or sensor artefacts. Such changes are important to identify, and our approach allows their automation and, if necessary, in real-time. This means that EWS techniques could be used for condition monitoring of environmental sensor networks. This is a promising novel application of the tipping point analysis in a new domain.

Acknowledgement

This work was funded by the UK Government's Department for Science, Innovation & Technology (DSIT) through the UK's National Measurement System programmes. Kate Willett was supported by the Met Office Hadley Centre Climate Programme funded by DSIT.



4.1 Code/Data availability

The code is based on the autocorrelation function that is available in any programming language. The data is property of Met Office UK.

210 **4.2 Author contribution**

The authors contributed equally to manuscript development.

4.3 Competing interests

The authors declare that they have no conflict of interest.



References

- 215 Brockwell P. and R. Davis, Introduction to Time Series and Forecasting, Springer Texts in Statistics, 2016.
- Broomhead, D. and G. King. *On the Qualitative Analysis of Experimental Dynamical Systems*. In book: Nonlinear Phenomena and Chaos, Malvern Physics Series. Publisher: Adam Hilger Ltd, Bristol Editors: E. Pike, S. Sarkar, 1986.
- Brugnara, Y., McCarthy, M. P., Willett, K. M., & Rayner, N. A., Homogenization of daily temperature and humidity series in the UK. *International Journal of Climatology* 43(4), 1693-1709, 2023.
- 220 Dakos, V, et al. Methods for Detecting Early Warnings of Critical Transitions in Time Series Illustrated Using Simulated Ecological Data, *PLoS ONE* 7 (7), e41010, 2012.
- Gladwell M. The Tipping Point: How Little Things Can Make a Big Difference. *Little Brown*, 2000.
- Held, H. and T Kleinen. Detection of climate system bifurcations by degenerate fingerprinting, *GRL* 31 (23), L23207, 2004.
- Hersbach H, Bell B, Berrisford P, et al. The ERA5 global reanalysis. *Q J R Meteorol Soc.* 146, 1999-2049, 2020.
- 225 Lenton, T, et al. Tipping elements in the Earth's climate system, *Proceedings of the National Academy of Sciences USA* 105 (6), 1786-1793, 2008.
- Lenton T., V. N. Livina, V. Dakos, E. H. van Nes and M. Scheffer, Early warning of climate tipping points from critical slowing down: comparing methods to improve robustness, *Phil. Trans. R. Soc. A* 370, 1185-1204, 2012.
- Livina, V, and T Lenton. A modified method for detecting incipient bifurcations in a dynamical system, *Geophys. Res. Lett.* 34, L03712, 230 2007.
- Livina, V, F Kwasniok, and T Lenton. Potential analysis reveals changing number of climate states during the last 60 kyr, *Climate of the Past* 6, 77-82, 2010.
- Livina, V, F Kwasniok, G Lohmann, J Kantelhardt, and T Lenton. Changing climate states and stability: from Pliocene to present, *Climate Dynamics* 37 (11-12), 2437-2453, 2011.
- 235 Livina, V, P Ditlevsen, and T Lenton. An independent test of methods of detecting system states and bifurcations in time-series data, *Physica A* 391 (3), 485-496, 2012.
- Livina, V, G Lohmann, M Mudelsee, and T Lenton. Forecasting the underlying potential governing the time series of a dynamical system, *Physica A* 392 (18), 3891-3902, 2013.
- Livina V., E. Barton, and A. Forbes, Tipping point analysis of the NPL footbridge, *Journal of Civil Structural Health Monitoring* 4, 91-98, 240 2014.
- Livina V. et al, Tipping point analysis of electrical resistance data with early warning signals of failure for predictive maintenance, *Journal of Electronic Testing* 36, 569-576, 2020.
- Livina V., Network analysis: Connected climate tipping elements, *Nature Climate Change* 13, 15-16, 2023.
- Menne, M. J. and Williams Jr., C. N. Homogenization of temperature series via pairwise comparisons, *J. Climate*, 22, 1700-1717, 2009.
- 245 Peng C.-K., Buldyrev S. V., Havlin S., Simons M., Stanley H. E., Goldberger A. L. (1994), Mosaic organization of DNA nucleotides. *Phys. Rev. E* 49, 1685-1689.
- Peterson, T. C., Easterling, D. R., Karl, T. R., Groisman, P., Nicholls, N., Plummer, N., Torok, S., Auer, I., Boehm, R., Gullett, D., Vincent, L., Heino, R., Tuomenvirta, H., Mestre, O., Szentimrey, T., Salinger, J., Forland, E. J., Hanssen-Bauer, I., Alexandersson, H., Jones, P., and Parker, D., Homogeneity adjustments of in situ atmospheric climate data: a review, *Int. J. Climatol.*, 18, 1493-1517, 1998.
- 250 Poincaré H., Les Methodes Nouvelles de la Mecanique Celeste, v. 1, *Gauthier-Villars*, Paris, 1892.



- Reeves S., J., Chen, J., Wang, X. L., Lund, R., and Lu, Q. Q., A review and comparison of changepoint detection techniques for climate data, *J. Appl. Meteorol. Clim.*, 46, 900-915, 2007.
- Trewin, B. A daily homogenized temperature data set for Australia, *Int. J. Climatol.* 33, 1510-1529, 2013.
- Vaz Martins, T, V Livina, A Majtey, and R Toral, Resonance induced by repulsive interactions in a model of globally coupled bistable systems, *Phys. Rev. E* 81, 041103, 2010.
- 255 Willett K. M., R. J. H. Dunn, P. W. Thorne, S. Bell, M. de Podesta, D. E. Parker, P. D. Jones, and C. N. Williams Jr., HadISDH land surface multi-variable humidity and temperature record for climate monitoring, *Clim. Past* 10, 1983-2006, 2014.
- Wissel, C. A universal law of the characteristic return time near thresholds. *Oecologia* 65, 101-107, 1984. <https://doi.org/10.1007/BF00384470>
- 260 Zhao K., M.Wulder, T.Hu, R.Bright, Q.Wu, H.Qin, Y.Li, E.Toman, B.Mallick, X.Zhang, M.Brown, Detecting change-point, trend, and seasonality in satellite time series data to track abrupt changes and nonlinear dynamics: A Bayesian ensemble algorithm, *Remote Sensing of Environment* 232, 111181, 2019.



Appendix

We summarise the analysis in the Table and provide further illustrations from several other stations.

| N | Station | Year of detected change | Likely cause |
|----|-------------------------------|-------------------------|--------------|
| 1 | Aberporth | 2011 | climatic |
| 2 | Aldergrove | 1984, 1989 | instrumental |
| 3 | Baltasound | - | - |
| 4 | Benson | 2004, 2006, 2019 | climatic |
| 5 | Bingley | 1994, 1997 | instrumental |
| 6 | Boscombe Down | 2008, 2013 | climatic |
| 7 | Brize Norton | 1982, 1989 | instrumental |
| 8 | Camborne | 1995 | instrumental |
| 9 | Carlisle | 2011 | climatic |
| 10 | Chivenor | 1995, 2004, 2006, 2013 | climatic |
| 11 | Coningsby | 1983 | instrumental |
| 12 | Cranwell | 1996 | instrumental |
| 13 | Culdrose | - | - |
| 14 | Dyce | 1982 | instrumental |
| 15 | Eskdalemuir | 1984 | instrumental |
| 16 | Exeter | - | - |
| 17 | Fair Isle | - | - |
| 18 | Fylingdales | - | - |
| 19 | Guernsey | - | - |
| 20 | Heathrow | 1982 | instrumental |
| 21 | Hereford-Credenhill | 2005 | climatic |
| 22 | Inverness | 1995, 2000 | climatic |
| 23 | Isle of Portland | 1998, 1999 | instrumental |
| 24 | Jersey | 2001 | climatic |
| 25 | Kinloss | 2017, 2018 | climatic |
| 26 | Kirkwall | - | - |
| 27 | Langdon Bay | 1989 | instrumental |
| 28 | Leeming | - | - |
| 29 | Lerwick | - | - |
| 30 | Leuchars | 1983 | instrumental |
| 31 | Linton on Ouse | - | - |
| 32 | Lossiemouth | 2006, 2008 | climatic |
| 33 | Lyneham | - | - |
| 34 | Machrihanish | 2014, 2016, 2017 | climatic |
| 35 | Manston | 1982 | instrumental |
| 36 | Marham | - | - |
| 37 | Middle Wallop | 1988 | instrumental |
| 38 | Milford Haven Conservancy Boa | 2007 | climatic |
| 39 | Mumbles Head | 2011, 2015 | climatic |
| 40 | Northolt | 1984 | instrumental |
| 41 | Nottingham-Watnall | - | - |
| 42 | Odiham | 1988, 1995, 2007 | instrumental |
| 43 | Plymouth-Mountbatten | 2014 | climatic |
| 44 | Portglenone | 2007 | climatic |
| 45 | Scampton | 2018 | climatic |
| 46 | Shawbury | - | - |
| 47 | Shoeburyness-Landwick | 1985 | instrumental |
| 48 | Tiree | - | - |
| 49 | Valley | 1980 | instrumental |
| 50 | Waddington | 1982, 2004, 2008 | instrumental |
| 51 | Wattisham | 1989 | instrumental |
| 52 | Wick | - | - |
| 53 | Wight - St. Catherines Point | 2001 | instrumental |
| 54 | Wittering | 2020, 2021 | climatic |
| 55 | Yeovilton | 1995, 1998, 2010, 2016 | climatic |

Table A1. Detection of changes in the UK relative humidity records.

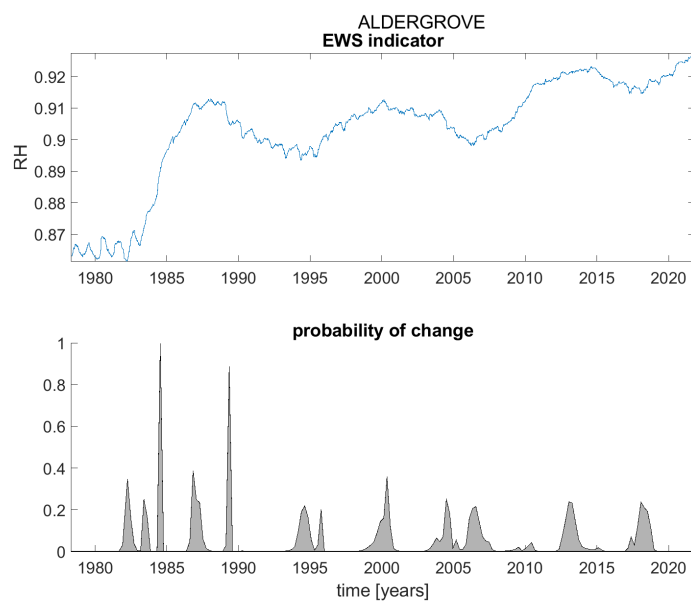


Figure A1. ACF(1) indicator (upper panel) and probability of detection of changes in the ACF(1) indicator (lower panel) for station Aldergrove.

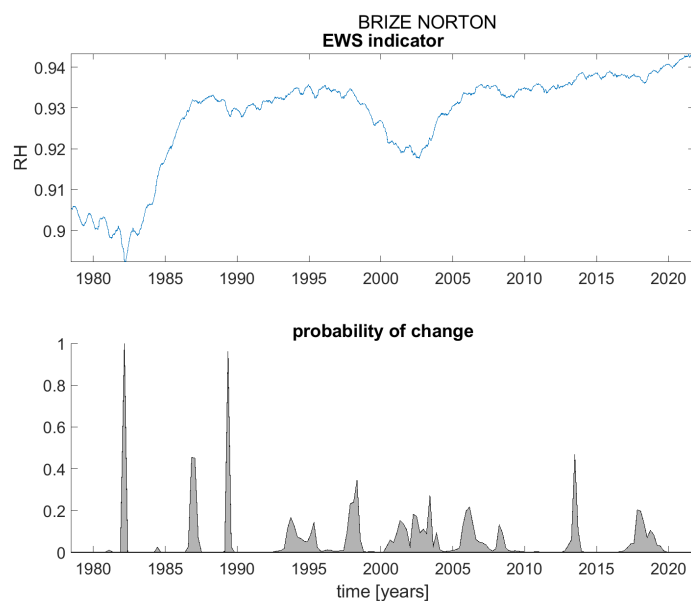


Figure A2. ACF(1) indicator (upper panel) and probability of detection of changes in the ACF(1) indicator (lower panel) for station Brize Norton.

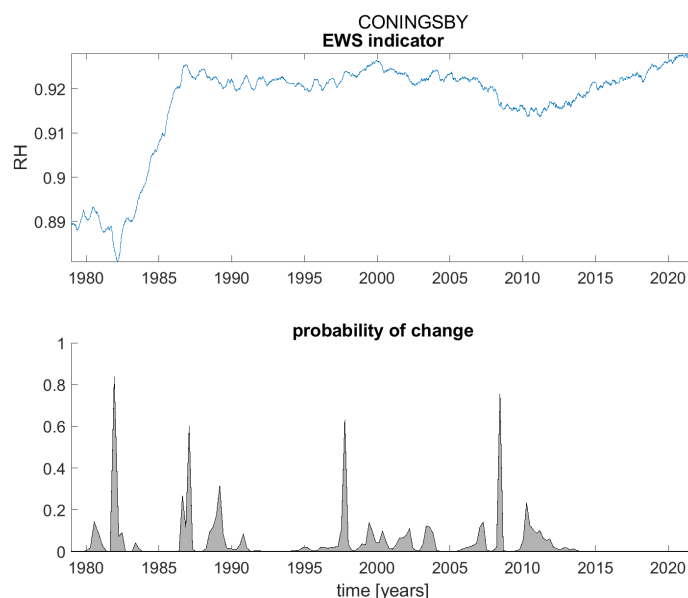


Figure A3. ACF(1) indicator (upper panel) and probability of detection of changes in the ACF(1) indicator (lower panel) for station Coningsby.

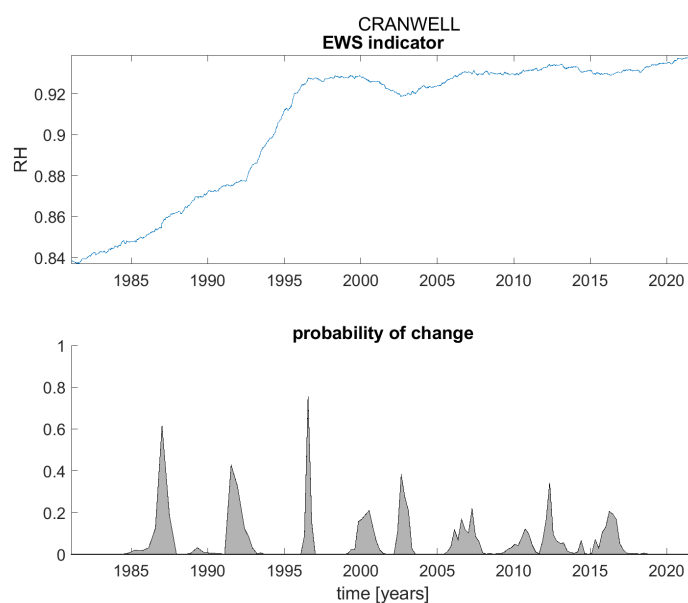


Figure A4. ACF(1) indicator (upper panel) and probability of detection of changes in the ACF(1) indicator (lower panel) for station Cranwell.

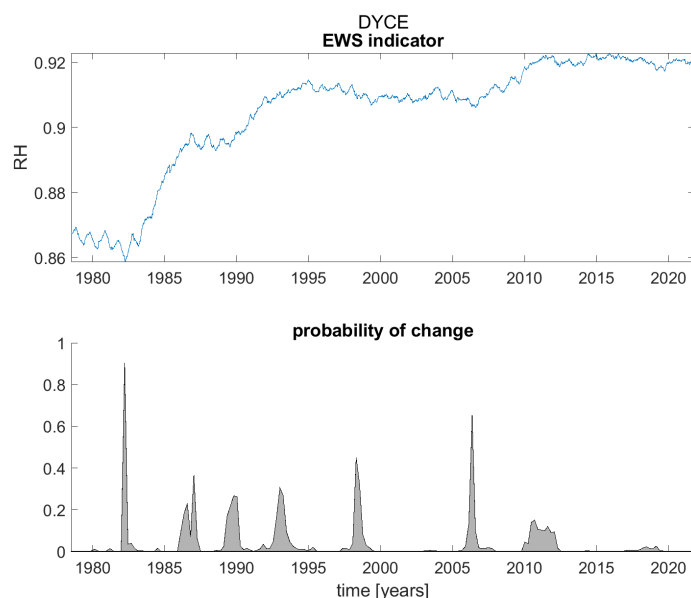


Figure A5. ACF(1) indicator (upper panel) and probability of detection of changes in the ACF(1) indicator (lower panel) for station Dyce.

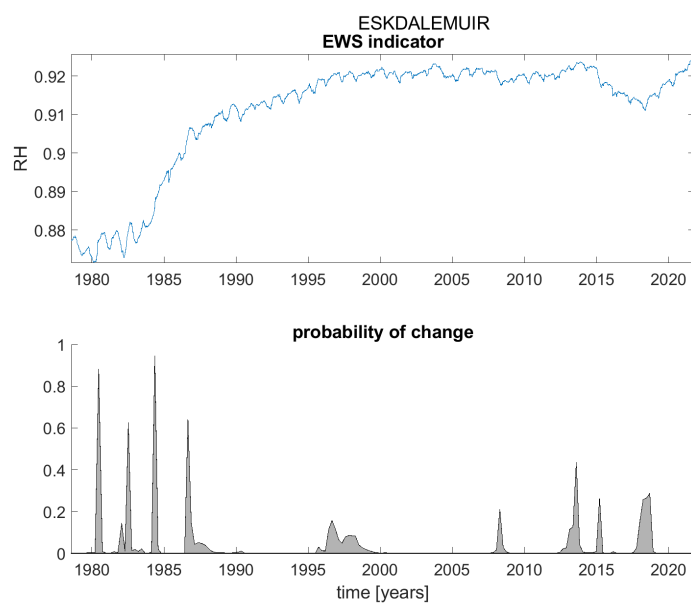


Figure A6. ACF(1) indicator (upper panel) and probability of detection of changes in the ACF(1) indicator (lower panel) for station Eskdalemuir.

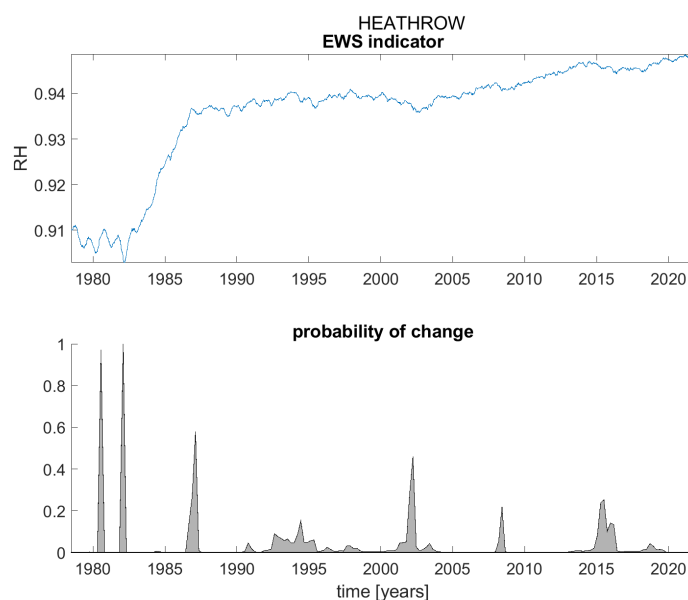


Figure A7. ACF(1) indicator (upper panel) and probability of detection of changes in the ACF(1) indicator (lower panel) for station Heathrow.

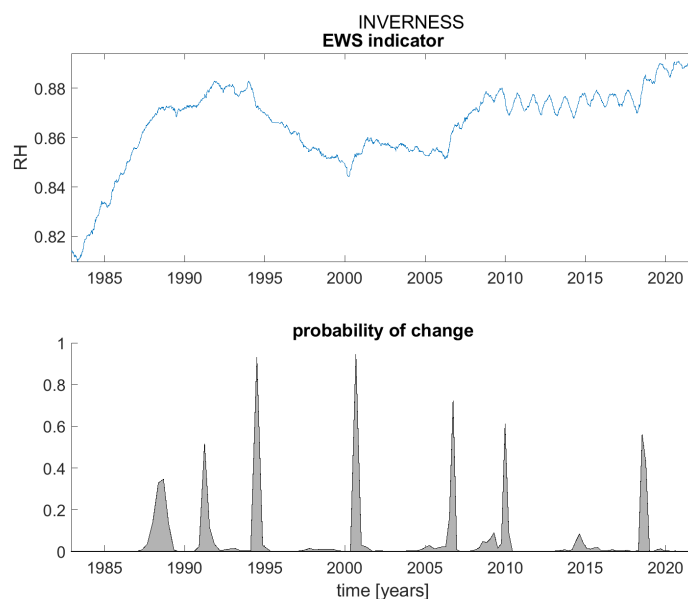


Figure A8. ACF(1) indicator (upper panel) and probability of detection of changes in the ACF(1) indicator (lower panel) for station Inverness.

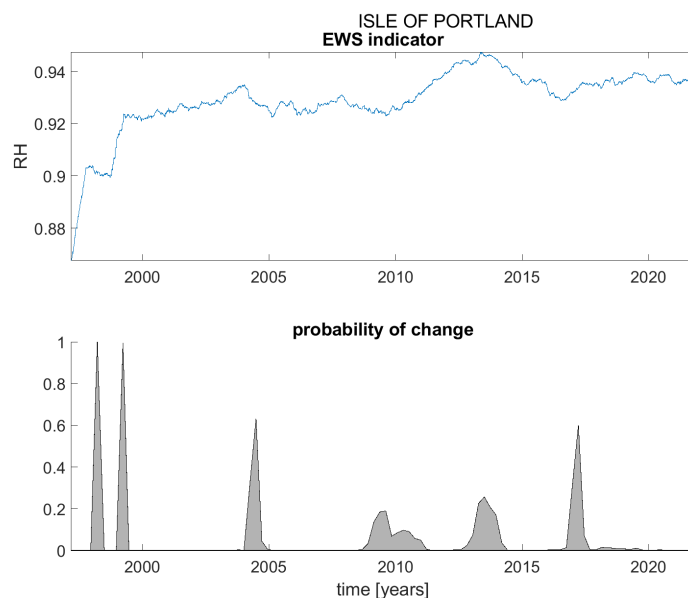


Figure A9. ACF(1) indicator (upper panel) and probability of detection of changes in the ACF(1) indicator (lower panel) for station Isle of Portland.

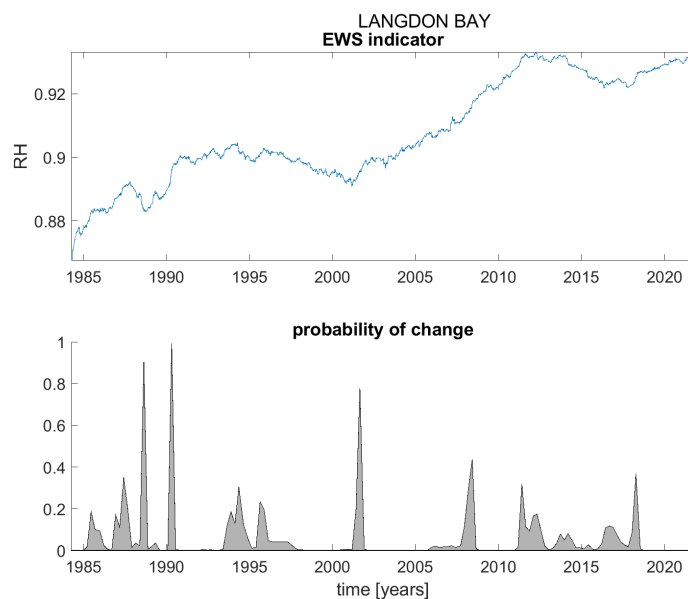


Figure A10. ACF(1) indicator (upper panel) and probability of detection of changes in the ACF(1) indicator (lower panel) for station Langdon Bay.

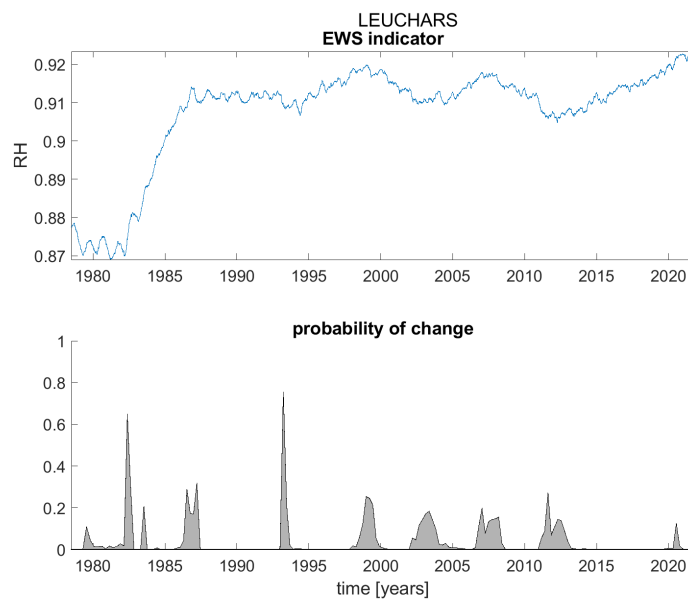


Figure A11. ACF(1) indicator (upper panel) and probability of detection of changes in the ACF(1) indicator (lower panel) for station Leuchars.

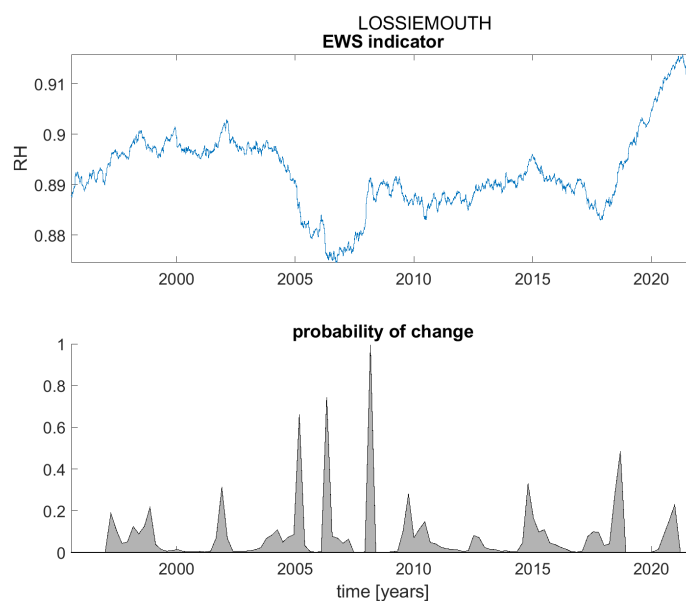


Figure A12. ACF(1) indicator (upper panel) and probability of detection of changes in the ACF(1) indicator (lower panel) for station Lossiemouth.

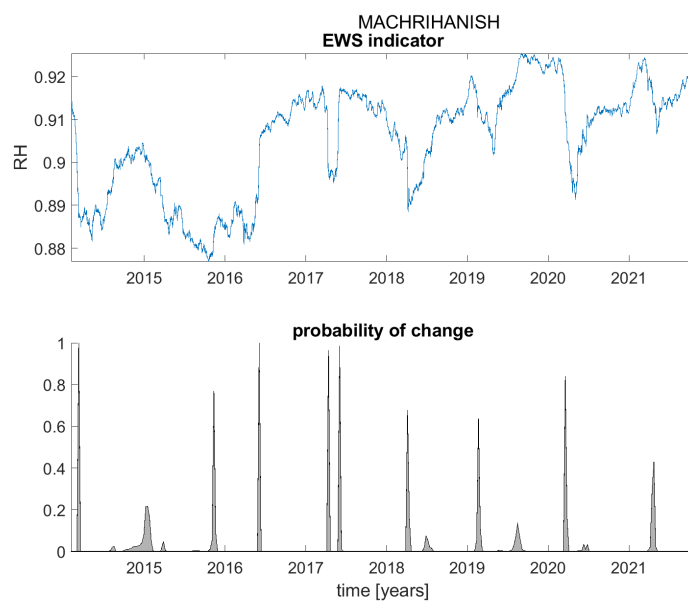


Figure A13. ACF(1) indicator (upper panel) and probability of detection of changes in the ACF(1) indicator (lower panel) for station Machrihanish.

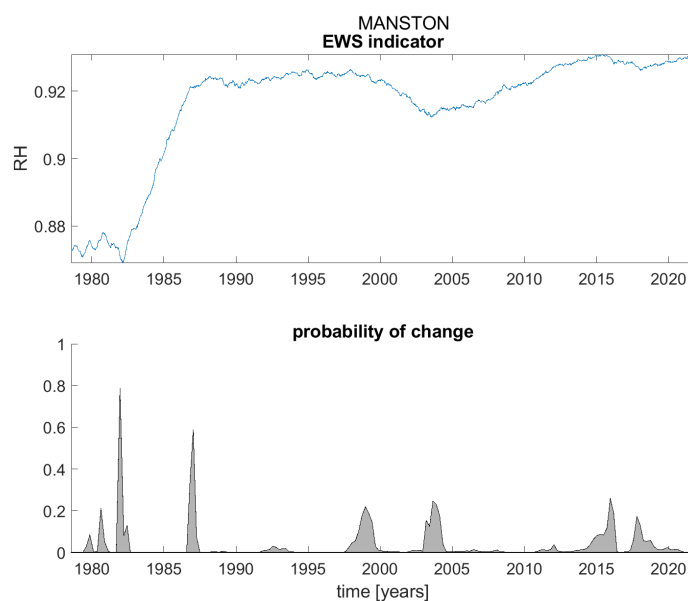


Figure A14. ACF(1) indicator (upper panel) and probability of detection of changes in the ACF(1) indicator (lower panel) for station Manston.

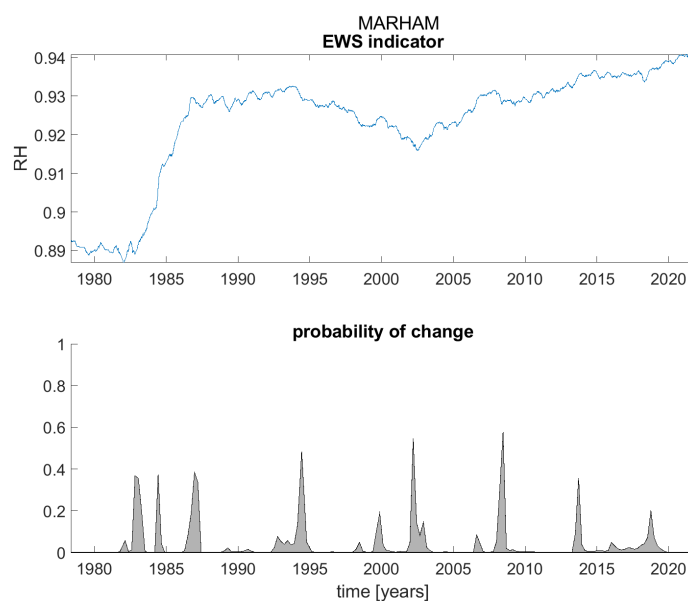


Figure A15. ACF(1) indicator (upper panel) and probability of detection of changes in the ACF(1) indicator (lower panel) for station Marham.

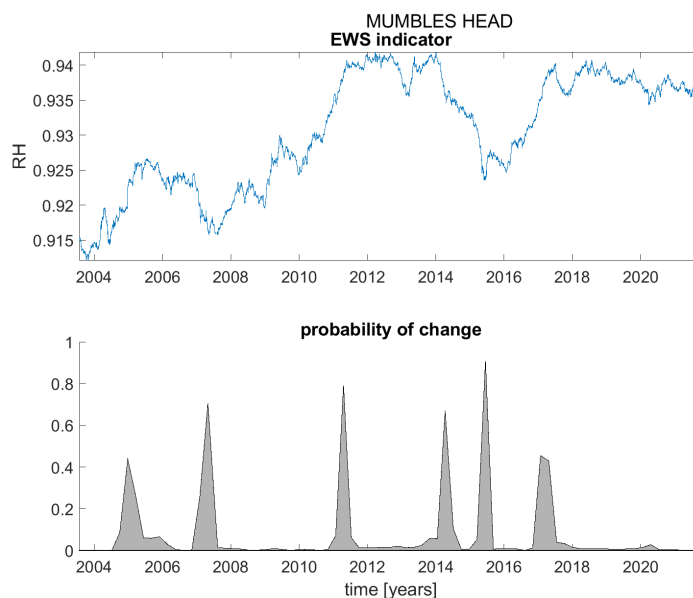


Figure A16. ACF(1) indicator (upper panel) and probability of detection of changes in the ACF(1) indicator (lower panel) for station Mumbles Head.

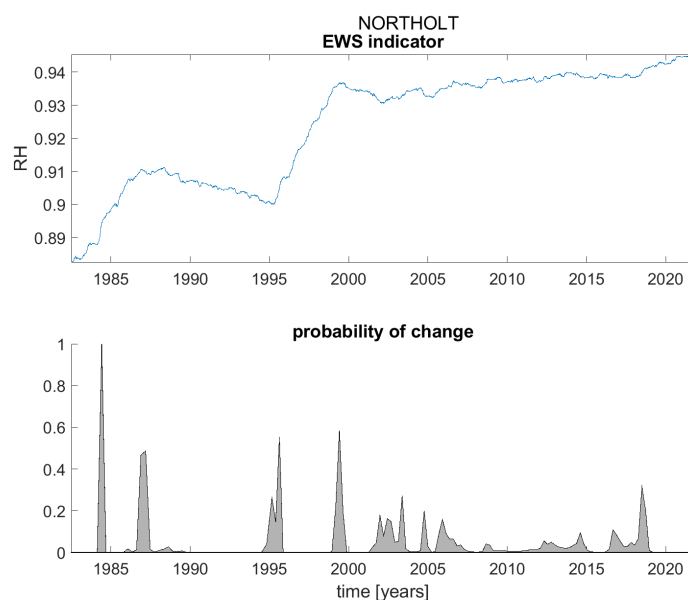


Figure A17. ACF(1) indicator (upper panel) and probability of detection of changes in the ACF(1) indicator (lower panel) for station Northolt.

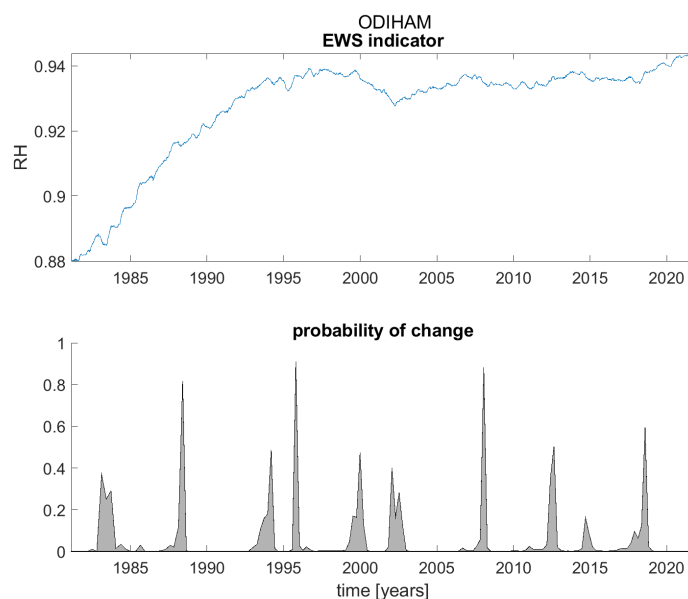


Figure A18. ACF(1) indicator (upper panel) and probability of detection of changes in the ACF(1) indicator (lower panel) for station Odiham.

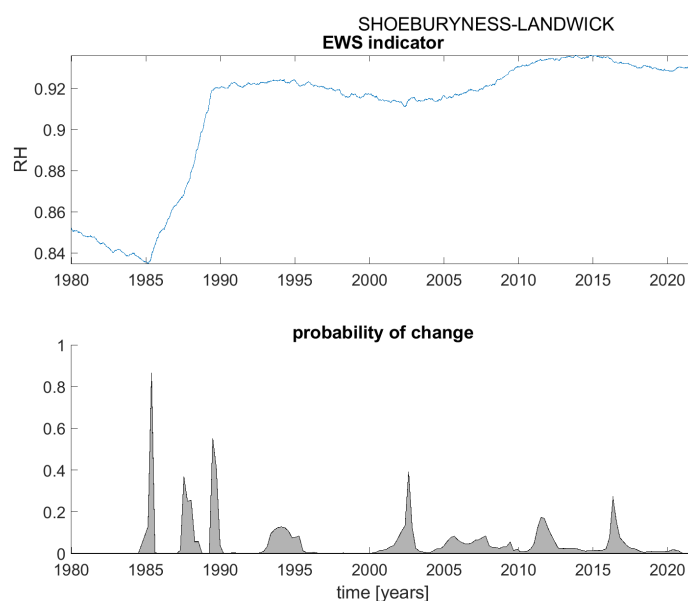


Figure A19. ACF(1) indicator (upper panel) and probability of detection of changes in the ACF(1) indicator (lower panel) for station Shoeburyness-Landwick.

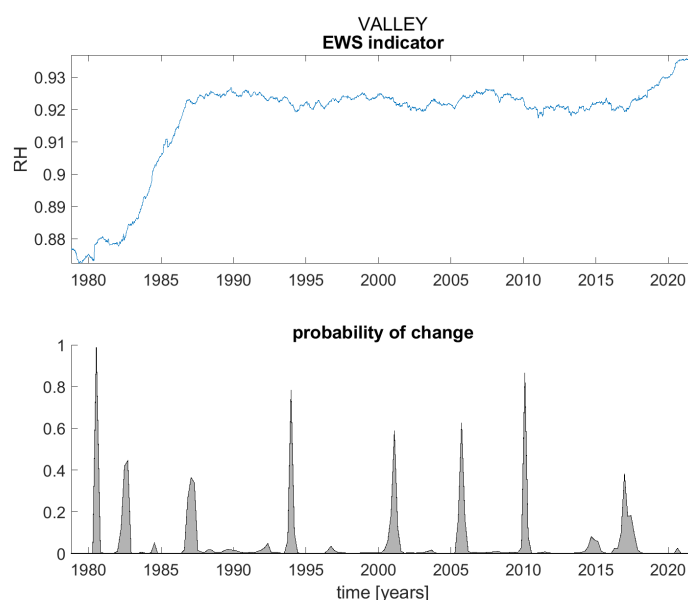


Figure A20. ACF(1) indicator (upper panel) and probability of detection of changes in the ACF(1) indicator (lower panel) for station Valley.

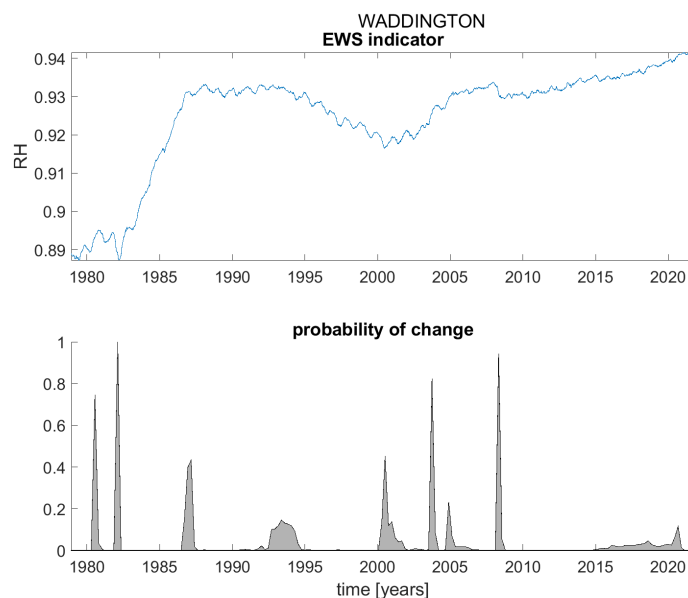


Figure A21. ACF(1) indicator (upper panel) and probability of detection of changes in the ACF(1) indicator (lower panel) for station Waddington.

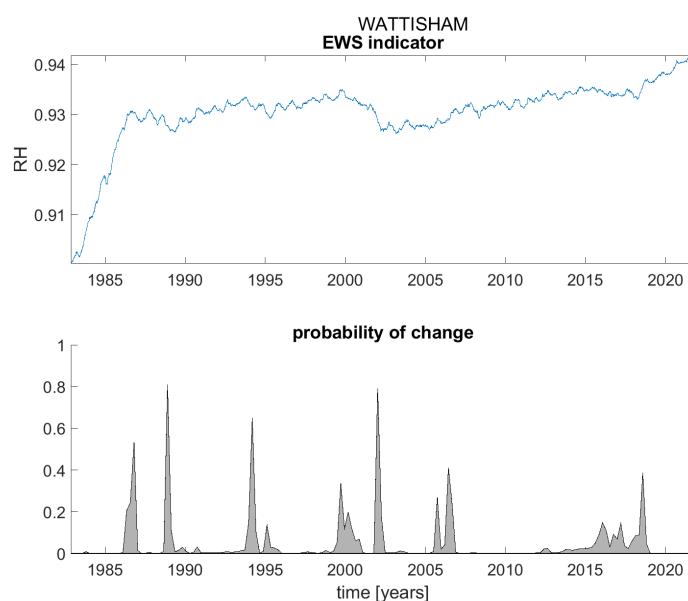


Figure A22. ACF(1) indicator (upper panel) and probability of detection of changes in the ACF(1) indicator (lower panel) for station Wattisham.